RESEARCH ARTICLE | NOVEMBER 02 2020

Bimetallic cluster film formation of Al and Mg with Cu investigated via He droplet deposition FREE

Claron J. Ridge ✉; Kyle R. Overdeep; Samuel B. Emery; Yan Xin; Robert J. Buszek; Jerry A. Boatz; C. Michael Lindsay

AIP Conf. Proc. 2272, 050026 (2020)
https://doi.org/10.1063/12.0000879

Bimetallic Cluster Film Formation of Al and Mg with Cu Investigated via He Droplet Deposition

Claron J. Ridge[1, a)], Kyle R. Overdeep[1], Samuel B. Emery[2], Yan Xin[3], Robert J. Buszek[4], Jerry A. Boatz[5], and C. Michael Lindsay[6]

[1]*UDRI, Energetic Materials Branch, 2306 Perimeter Rd., Eglin AFB, FL 32542,USA*
[2]*Naval Surface Warfare Center Indian Head EOD Tech. Div., 3196 Deep Point Ct., Indian Head, MD 20640, USA*
[3]*National High Magnetic Field Laboratory, Florida State University, Tallahassee, FL 32310, USA*
[4]*ERC Inc. Edwards AFB, CA 93524, USA*
[5]*Air Force Research Laboratory, Aerospace Systems Directorate, Edwards AFB, CA 93524, USA*
[6]*Air Force Research Laboratory, Munitions Directorate, 2306 Perimeter Rd., Eglin AFB, Florida 32542, USA*

[a)]Corresponding author: claron.ridge.ctr@us.af.mil

Abstract. In an effort to probe the interactions of reactive materials at the nanoscale the formation of bimetallic cluster films has been investigated via He droplet mediated deposition and transmission electron microscopy. Cu-Mg core-shell clusters are shown to have a distinct behavior from core-shell inverted Mg-Cu clusters. Mg undergoes Ostwald ripening if it is deposited as the shell material which does not occur for core-shell inverted clusters. Additionally, Al-Cu core-shell clusters appear to undergo both core-shell structural inversion and oxidative etching of the Al shell once formed.

INTRODUCTION

Reactive bimetallic (i.e. intermetallics) and metal/metal oxide (i.e. thermites) materials are appealing systems for those interested in increasing the energy density and achieving higher reactive temperatures as compared to organic (carbon, nitrogen, oxygen, and hydrogen) based energetic materials. The main drawback of inorganic energetic materials is the relatively slow reaction rates which are limited by mass and thermal diffusion. Efforts to overcome this issue focus on decreasing the length scale between reactants from micrometers to nanometers to reduce the diffusion distance down toward the molecular scale [1]. Moving to the nanoscale introduces new challenges as the decreased length scales come with an increase in surface area and surface energy that shift the physical properties dramatically, often in ways that are difficult to predict. This research effort explores this problem by probing the interactions of bimetallic systems at the molecular scale.

To achieve the level of control necessary to build bimetallic systems with sub-nanometer domain lengths, clusters are formed atom by atom via He droplet mediated deposition (HDMD). This technique (first demonstrated by Mozhayskiy and coworkers) [2] exploits the superfluidity of He droplets to bring together atoms in a cold (~0.4 K) environment, which freezes out most reactions, and subsequently impinging the droplet beam onto a surface to soft land the resulting clusters for further investigation. This is, to our knowledge, the lowest energy pathway to aggregating atoms into clusters, and a number of studies confirm that clusters can be deposited without the high impact energies associated with other physical methods [3]. Sequential doping of the droplet beam will grow clusters layer by layer making it possible to construct core-shell configurations. This has been demonstrated by several research groups with mostly coinage metals (see reference 4 and references therein). The technique is also suitable for making composite nanoparticles of molecular components if the molecular species have sufficient vapor pressure to be picked up by the droplets in the collision cell. Fomblin-Mg (a known pyrotechnic mixture) cluster films have been produced via HDMD in our lab, and the resulting film was shown to be in an unreacted state [5].

Shock Compression of Condensed Matter - 2019
AIP Conf. Proc. 2272, 050026-1–050026-5; https://doi.org/10.1063/12.0000879
Published by AIP Publishing. 978-0-7354-4000-5/$30.00

To gain further insight to the reactivity of inorganic energetic materials, reactive constituents are brought together in this low energy environment into core-shell arrangements with domain sizes from 0.3 to 5 nm (i.e., single atomic layers to nanoclusters). In this effort we have doped He droplets with combinations of Mg, Al, and Cu. In a previous study we reported on the sintering of Mg clusters deposited via HDMD showing that they undergo Ostwald ripening, resulting in large (100's of nanometers) islands and sheets on the amorphous carbon (a-C) substrate [6]. We subsequently found, unexpectedly, that Mg-Cu core-shell clusters formed in He droplets are subject to core-shell inversion [7]. The inversion process could be initiated inside the droplet, or after it is deposited, or after it is exposed to ambient atmosphere. The Mg appears to be almost completely oxidized, indicating that exposure to O_2 and H_2O may play a role in the inversion. However, *ab initio* DFT calculations indicate that there is a very small activation barrier (~0.5 kcal mol^{-1}) to Cu atoms diffusing into the Mg core indicating the inversion begins in the He droplet. In a follow up theoretical study, further DFT calculations showed that, in the reverse situation, Mg faced a much larger activation barrier to penetrating the Cu core (~6 kcal mol^{-1}) [8]. Experimental investigation of reverse order pickup (Cu picked up first) is presented in this work.

Al clusters deposited via HDMD have also been investigated in a recent report from our lab showing a surprising size dependent stability [9]. Al clusters smaller than ~4 nm are not stable on the surface and undergo oxidative etching leaving behind small traces of aluminum oxide but no clusters. Larger clusters appear to be stable on the surface even though they are completely oxidized. It is postulated that this phenomenon is caused by a steep drop off in the ratio of highly uncoordinated surface atoms to bulk atoms as the size increases. In this work we follow up these experiments by investigating Al-Cu core-shell clusters synthesized via HDMD.

METHODS

The experimental apparatus used in this study has been described in great detail elsewhere [10, 11]. In brief, a superfluid He droplet beam is produced by expanding chromatographic grade He gas (99.9999% purity) into high vacuum chamber (base pressure of $1x10^{-8}$ torr rising to $1x10^{-7}$ to $1x10^{-5}$ torr during deposition) through a cryogenically cooled (4-50 K) Pt aperture (~5 μm dia.) at a stagnation pressure of up to 100 bar (see Fig. 1). The beam is defined by a 0.5 mm skimmer 1.7 cm downstream from the nozzle which is also the entrance to a second vacuum chamber containing the doping cells. The second chamber is separated from a third chamber by a gate valve. The third chamber contains a quadrapole mass spectrometer (QMS) (Extrel inc.) with a 3 mm entrance aperture ~85 cm downstream from the nozzle. The base pressure in both the second and third chamber is $2x10^{-9}$ torr, rising up to $1x10^{-6}$ torr under high throughput He beam conditions. The nozzle is mounted on a translation stage to align the beam to the axis defined by the skimmer and QMS by maximize the 8 amu (He_2) signal in the QMS.

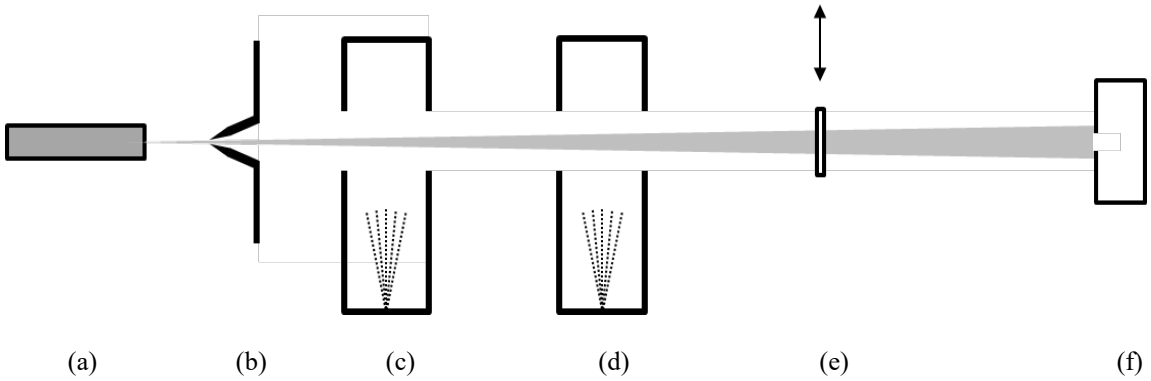

FIGURE 1. Diagram of the experimental apparatus. (a) Cryogenically cooled (4 to 50 K) He nozzle consisting of a 5 micron aperture. (b) 0.5 mm skimmer 1.7 cm from the nozzle. (c) & (d) Effusive ovens contained in shielded collision zones that are 7 cm in width. (e) Translational stage for moving samples into the path of the He beam. (f) Ionization region of the QMS analyzer with a 3 mm aperture centered on the beam path.

The He droplets can be doped by passing the beam through doping cells consisting of high temperature effusion ovens mounted orthogonally to the He beam and surrounded by stainless steel shielding to prevent cross-contamination from one cell to another. Mounted opposite each effusion oven is a quartz crystal microbalance (QCM)

to monitor their output. Cu and Al are doped into the beam via high temperature ovens loaded with 99.97% Cu shot (Alfa Aesar) or 99.99% Al pellets (Kurt J. Lesker). Mg (99.98%, Aldrich) is doped from a similar oven, but operated at much lower temperatures with a steel crucible with a 1 mm aperture to limit the Mg vapor beam. Nanoparticles are deposited onto ultrathin amorphous carbon (a-C) supported on 400 mesh Au TEM grids (Ted Pella inc., pro. no. 01824g) that are mounted on a translator that can move the samples into the path of the beam ~70 cm downstream from the nozzle. After deposition, samples are removed from vacuum and transferred under ambient conditions for TEM analysis. TEM is performed in an aberration corrected JEOL 2100F TEM operating at 200 keV. Scanning transmission electron microscopy (STEM) was collected using high angle annular dark field (HAADF) imaging which produces a bright field image where the higher contrast is associated with higher atomic *Z* number (TEM is a dark field where higher *Z* materials appear darker). Electron energy loss spectroscopy (EELS) mapping was also performed in the TEM instrument to map out Cu, Mg, Al, and O. X-ray photoelectron spectroscopy (XPS) samples were deposited onto 10×10×0.5 mm Si 100 substrates (MTI, n-type undoped) and shipped to a separate analysis lab.

RESULTS

To gain insight on the previous results with Mg-Cu core-shell inversion, we have deposited clusters made with the reverse doping order where Cu was picked up first in the droplets. The expected size of clusters formed in a He droplet at a particular size can be calculated from Equation 1,

$$z = \sigma n l g \tag{1}$$

where z is the average collision number, σ the collisional cross-section, n the dopant number density, l is the interaction path length, and g is the correction factor for the relative velocity of droplet to dopant. The average size of the droplets, and therefore the cross-section, can be estimated from experimental conditions, namely, nozzle temperature, aperture size, and stagnation pressure (for a detailed explanation see references 11 and 12). The dopant number density can be determined from the oven flux which is measured with a QCM. If the binding energy associated with the formation of the metal cluster is large compared to the cohesive energy of the droplet then one must take into account the decrease in droplet cross-section resulting from evaporative dissipation of the metal cluster binding energy. The path length is 7 cm. The correction factor for the relative velocity, g, can be obtained from reference 13, assuming a Boltzmann distribution of velocities for the dopants and droplet velocities from reference 12.

Taking these factors into account, experimental conditions can be adjusted to target an average metal cluster size. Here we targeted doping rates similar to those from reference 7. In that work ~2500 Mg atoms were picked up first, followed by ~730 Cu atoms. In this work ~1000 Cu atoms were picked up first followed by ~1200 Mg atoms. The width and shape of the distribution can also be estimated from experimental conditions (for specific details see references 11 & 12) and, for the parameters used in this work, result in a variation about the mean cluster diameter of ±30%.

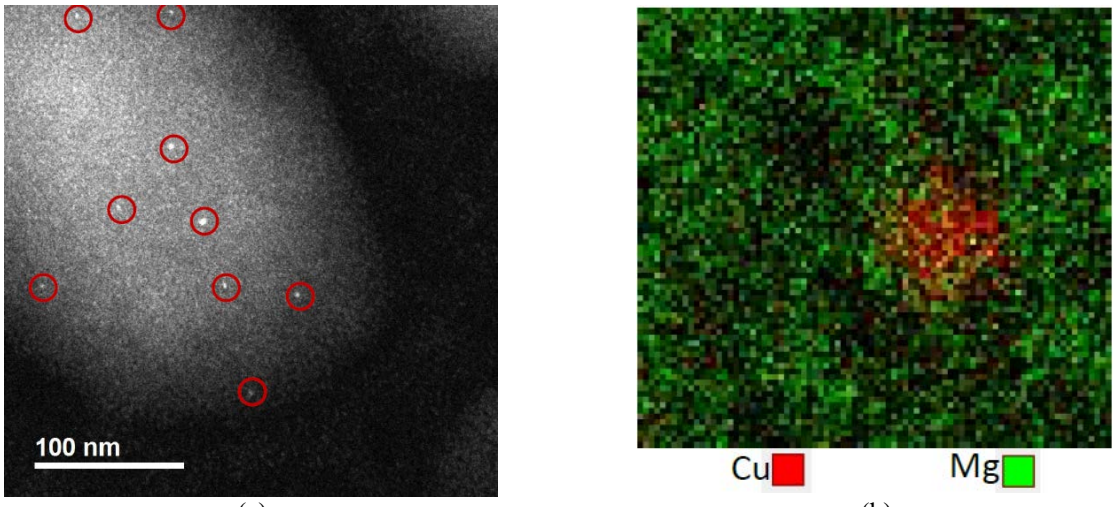

(a) (b)

FIGURE 2. (a) STEM bright field image of a large sintered Mg (magnesium oxide) island with Cu clusters (circled in red) embedded throughout. (b) EELS elemental map showing a 4 nm copper (red) cluster embedded in Mg (green).

STEM bright field images and elemental mapping of the Cu-Mg cluster deposition are shown in Fig. 2a & 2b, respectively. The STEM image shows a distribution of bright clusters embedded in large sheet-like islands. The EELS map confirms that the bright clusters are indeed Cu clusters (2 to 4 nm diameter, in reasonable agreement with the estimated cluster size) and the islands are MgO. XPS on similar depositions show chemical shifts of the Mg signal associated with MgO and MgC_2. The TEM substrates are a-C so it was not possible to do elemental mapping of the C but it can be assumed that the Mg reacts readily with C and O containing contaminants.

The images indicate the Mg, when deposited as the shell of the core-shell arrangement, Ostwald ripens (atomic diffusion on the surface favors larger clusters, so large clusters grow into sheets while smaller cluster disappear) in a similar fashion to our previous work in which small Mg clusters are deposited alone [6]. This is in contrast with the results from Mg-Cu core-shell depositions in which the Mg core inverted to the Mg shell but did not further ripen into islands.

The doping order dependent behavior observed here suggests that the Mg core of the Mg-Cu core-shell must not be fully inverted while in the droplet. This supports the theory that the core-shell does not fully invert until after deposition, possibly upon exposure to an oxidizing atmosphere when transferred. This theory is also supported by the results of Schnedlitz and coworkers [4], who found that Ni-Au core-shell clusters synthesized via HDMD undergo core-shell inversion when exposed to higher temperatures (400 °C) and the Ni oxidizes. Mg is more easily oxidized than Ni, so it is not surprising that higher temperatures do not appear to be needed for the oxidative induced core-shell inversion.

Al-Cu HDMD Core-Shell Clusters

The deposition of Al-Cu HDMD clusters is carried out in a similar fashion. The cluster size target for the Al, which was picked up first, was ~900 atoms which corresponds to a spherical cluster diameter of 2.7 nm. For the Cu shell, ~1000 atoms were picked up which, assuming a spherical core shell arrangement, would result in a 3.4 nm cluster. The TEM, STEM, and EELS map images appear in Fig. 3. A representative bright field TEM image (Fig. 3a) shows ~3 nm metal clusters dispersed on the a-C substrate. In higher contrast STEM images (Fig. 3b) atomic lattice patterns can be seen in the clusters with more amorphous material around the edges. The EELS map confirms that the clusters observed are Cu with no detectable quantity of Al present.

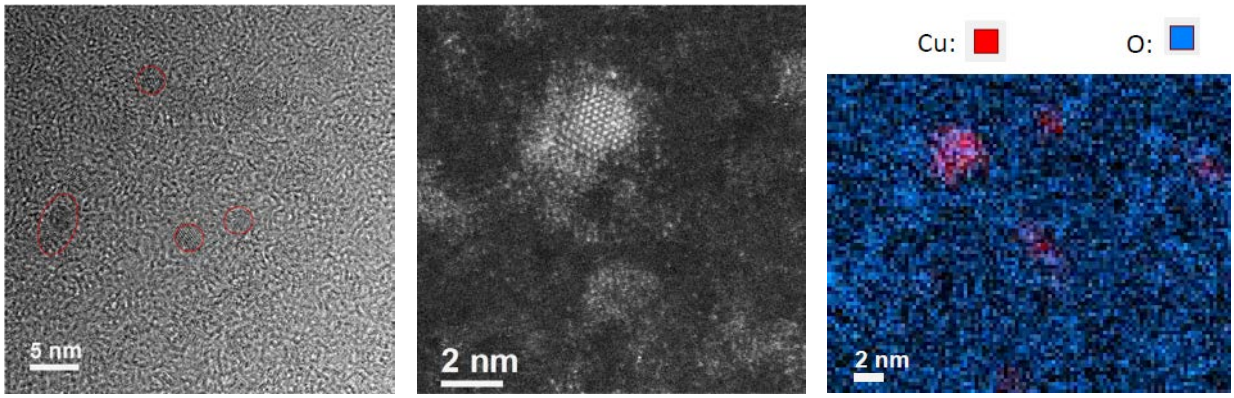

(a) (b) (c)

FIGURE 3. (a) TEM image of Al-Cu HDMD clusters. Red circles indicate metal clusters (b) STEM image showing a crystalline Cu clusters. (c) EELS map of Cu (red) and O (blue). Al signal was too weak to be detected. The surface of the Cu clusters appears to be partially oxidized.

The absence of Al is consistent with our previous experiments. It has been shown in our previous work [7] that a metal core with a relatively high oxidative potential will readily undergo core-shell inversion. Al not only has a high oxidative potential but, as we have seen in our recent work [9], it can be oxidatively etched if it is at the surface of a cluster smaller than 4 nm in diameter. Under the doping conditions of this experiment, the core-shell clusters would be ~3.4 nm and so if the Al-Cu core-shell undergoes inversion then it is in the size range where the surface Al will be subject to oxidative etching.

CONCLUSIONS

The unusual behavior of core-shell metal clusters synthesized via HDMD have been investigated via electron microscopy. The results are consistent and build upon observations from previous work:

- Mg, when deposited as a thin shell constituent, undergoes Ostwald ripening unperturbed by the presence of Cu core clusters.
- This result suggests a post-deposition mechanism for the Mg-Cu core-shell inversion seen in previous work.
- Al-Cu core-shell clusters undergo core shell inversion similar to that observed for Mg-Cu.
- The Al shell is subject to oxidative etching as long as the total cluster size < 4 nm.

Future work will focus on the interaction of other constituents with Al (Au, Si, organics, etc.) with the aim to create a stable Al core that does not invert and is protected from oxidation.

ACKNOWLEDGMENTS

The efforts conducted at Eglin Air Force Base were supported by the Air Force Office of Scientific Research under AFOSR Award No. 17RWCOR451. TEM work was performed at the National High Magnetic Field Laboratory of Florida State University, which is supported by the National Science Foundation Cooperative Agreement No. DMR-1157490, DMR-1644779, and the State of Florida.

REFERENCES

1. A. Rai, K. Park, L. Zhou, and M. R. Zachariah, Combust. Theory Model. **10**, 843 (2006).
2. V. Mozhayskiy, M. N. Slipchenko, V. K. Adamchuk, and A. F. Vilesov, J. Chem. Phys. **127**, 094701 (2007).
3. P. Thaler, A. Volk, D. Kenz, F. Lackner, G. Haberfehlner, J. Steurer, M. Schnedlitz, and W. E. Ernst, J. Chem. Phys. **143**, 134201 (2015).
4. M. Schnedlitz, M. Lasserus, R. Meyer, D. Knez, F. Hofer, W. E. Ernst and A. W. Hauser, Chem. Mater. **30**, 3, 1113-1120 (2018).
5. S. B. Emery, K. B. Rider, and C. M. Lindsay, Propel., Explos., Pyro. **39**, 161 (2014).
6. S. B. Emery, K. B. Rider, B. K. Little, A. M. Schrand, and C. M. Lindsay, J. Chem. Phys. **139**, 054307 (2013).
7. S. B. Emery, Y. Xin, C. J. Ridge, R. J. Buszek, J. A. Boatz, J. M. Boyle, B. K. Little, and C. M. Lindsay, J. Chem. Phys., **142** (8), 084307 (2015).
8. R. J. Buszek, C. J. Ridge, S. B. Emery, C. M. Linday, and J. A. Boatz, J. Phys. Chem. A, **120**, 9612−9617 (2016).
9. K. R. Overdeep, C. J. Ridge, Y. Xin, T. N. Jensen, S. L. Anderson, and C. M. Lindsay, J. Phys. Chem. C, **123**, 23721-23731 (2019)
10. R. M. Cleaver and C. M. Lindsay, Cryogenics **52**, 389 (2012).
11. S. B. Emery, K. B. Rider, B. K. Little, and C. M. Lindsay, J. Phys. Chem. C, **117**, 2358 (2013).
12. L. F. Gomez, E. Loginov, R. Sliter, and A. F. Vilesov, J. Chem. Phys. **135**, 154201 (2011).
13. K. Berkeling, R. Helbing, K. Kramer, H. Pauly, C. Schlier and P. Toschek, Z. Phys., **166**, 406 (1962).